

HETEROCYCLES, Vol. 90, No. 1, 2015, pp. 462 - 481. © 2015 The Japan Institute of Heterocyclic Chemistry
Received, 26th June, 2014, Accepted, 29th July, 2014, Published online, 19th August, 2014
DOI: 10.3987/COM-14-S(K)43

SYNTHESIS OF BICYCLIC DIOXETANES BEARING A HYDROXYPHENANTHRENE OR HYDROXY[4]HELICENE MOIETY AND THEIR BASE-INDUCED CHEMILUMINESCENT DECOMPOSITION

Yohei Koyama, Nobuko Watanabe, Hisako K. Ijuin, and Masakatsu
Matsumoto*

Department of Chemistry, Kanagawa University, Tsuchiya, Hiratsuka, Kanagawa
259-1293, Japan *E-mail address:* matsumo-chem@kanagawa-u.ac.jp

Abstract – Six bicyclic dioxetanes bearing a 1-hydroxyphenanthren-3-yl **2-iv**, 3-hydroxyphenanthren-1-yl **2-ov**, 4-hydroxyphenanthren-2-yl **2-oh**, 2-hydroxyphenanthren-4-yl **2-ih**, 4-hydroxy[4]helicen-2-yl **3-iv** and 2-hydroxy[4]helicen-4-yl group **3-ov** were synthesized and their base-induced chemiluminescent decomposition was investigated in a TBAF (tetrabutylammonium fluoride) / MeCN system. For dioxetanes in the *iv*-series **2-iv** and **3-iv** including α -naphthol-analog **17a** and those in the *ov*-series **2-ov** and **3-ov** including β -naphthol-analog **17b**, we investigated how the chemiluminescence properties changed with an increase in the number of fused benzene rings of a hydroxyarene moiety attached to a dioxetane ring. The results showed that a) maximum wavelength of chemiluminescence $\lambda_{\max}^{\text{CL}}$ tended to shift to a longer wavelength region as the number of fused benzene rings increased, b) the k^{CTID} values for the *iv*-series were >1000 times larger than those for the *ov*-series regardless of the number of fused benzene rings, and c) a dioxetane in the *iv*-series tended to have a higher singlet-chemiexcitation efficiency Φ_{S} than the corresponding dioxetane in the *ov*-series. This tendency could be explained by the “*syn/anti*” rotational isomerism of an aromatic electron donor, where an *anti*-rotamer gives Φ_{S} far more effectively than a *syn*-rotamer.

INTRODUCTION

A dioxetane bearing an aromatic electron donor such as oxidoaryl anion undergoes intramolecular charge-transfer-induced decomposition (CTID) with an accompanying emission of bright light.¹⁻⁶ This phenomenon has received considerable attention from the viewpoints of mechanistic interest related to bioluminescence and its potential for application to clinical and biological analysis.^{7,8} Thus, intensive studies have been conducted, and have shown that an aromatic electron donor significantly affects the

chemiluminescence properties such as the chemiluminescence spectrum, chemiluminescence efficiency and the rate of decomposition for CTID-active dioxetanes. Such effects are mainly due to the structure of the π -electron system and the bulkiness of the aromatic electron donor.

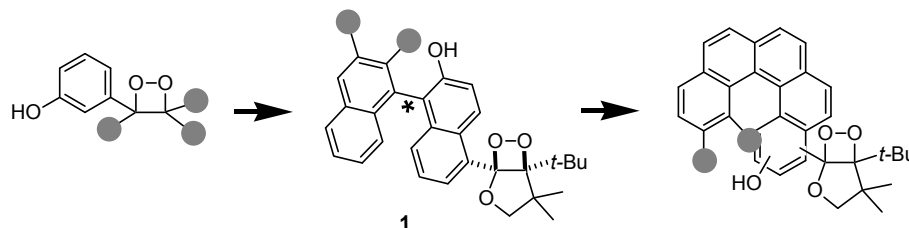


Figure 1. CTID-active dioxetanes bearing a chiral aromatic electron donor

On the other hand, the chirality of an aromatic electron donor such as a biaryl due to atropisomerism leads to unique chemiluminescence for a CTID-active dioxetane. For instance, optically active bicyclic dioxetanes **1** bearing a chiral binaphthyl moiety have very recently been found to show chiral-induced chemiluminescence in an optically anisotropic microenvironment (Figure 1).^{9,10} In addition to this phenomenon, it would be interesting to determine whether or not CTID of optically active dioxetanes shows the emission of polarized light. For observing such an unprecedented phenomenon, an important preliminary subject may be to design and synthesize dioxetanes bearing a helicene-type electron donor that could be expected to exhibit a large specific rotation due to its large helicity (Figure 1).

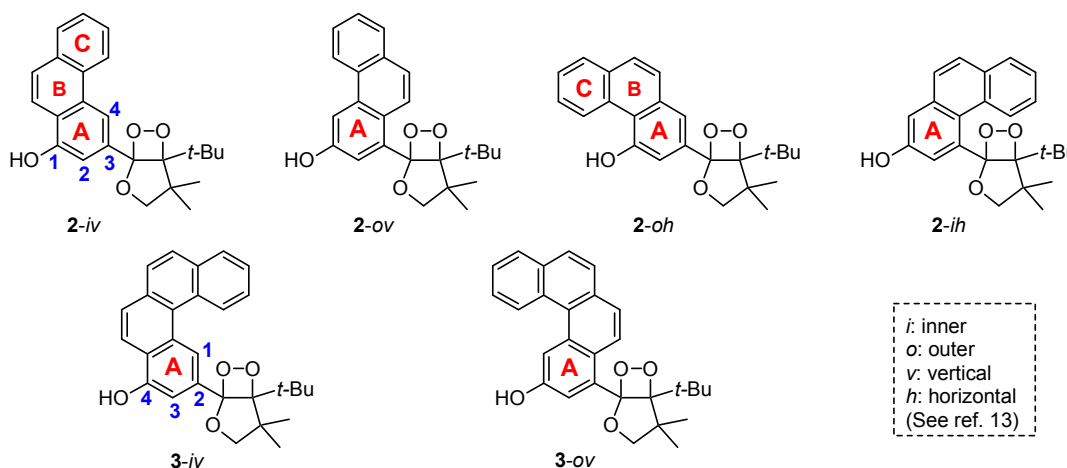


Figure 2. Bicyclic dioxetanes bearing a hydroxyphenanthrene or hydroxyl[4]helicene moiety

A promising candidate for such a CTID-active dioxetane would be one bearing a hydroxyhelicene moiety. However, there are too many substitution patterns when both a hydroxy group as a trigger and a dioxetane ring are introduced to an *ortho*-fused polyacene ring: there are 66 patterns for a [4]helicene (benzo[*c*]phenanthrene) and 91 for [5]helicene! Furthermore, little is currently known about the synthetic feasibility and chemiluminescence properties of a dioxetane bearing a helicene moiety. In light of the chemiluminescence properties for the CTID of dioxetanes bearing a hydroxynaphthyl group,¹¹ we decided to fundamentally investigate the CTID of racemic bicyclic dioxetanes bearing a phenanthrene

moiety in which both a hydroxy group and a dioxetane ring lie in an “*odd*” relationship on the A-ring.^{11,12} The thus-realized dioxetanes were **2-iv**, **2-ov**, **2-oh** and **2-ih**, as shown in Figure 2.¹³ Based on an evaluation with respect to the chemiluminescence properties, thermal stability, and synthetic feasibility of **2**, two selected dioxetanes bearing a hydroxyl[4]helicene moiety **3-iv** and **3-ov** were further synthesized and their CTID was investigated.

RESULTS AND DISCUSSION

Synthesis of bicyclic dioxetanes bearing a hydroxyphenanthrene or hydroxy[4]helicene moiety

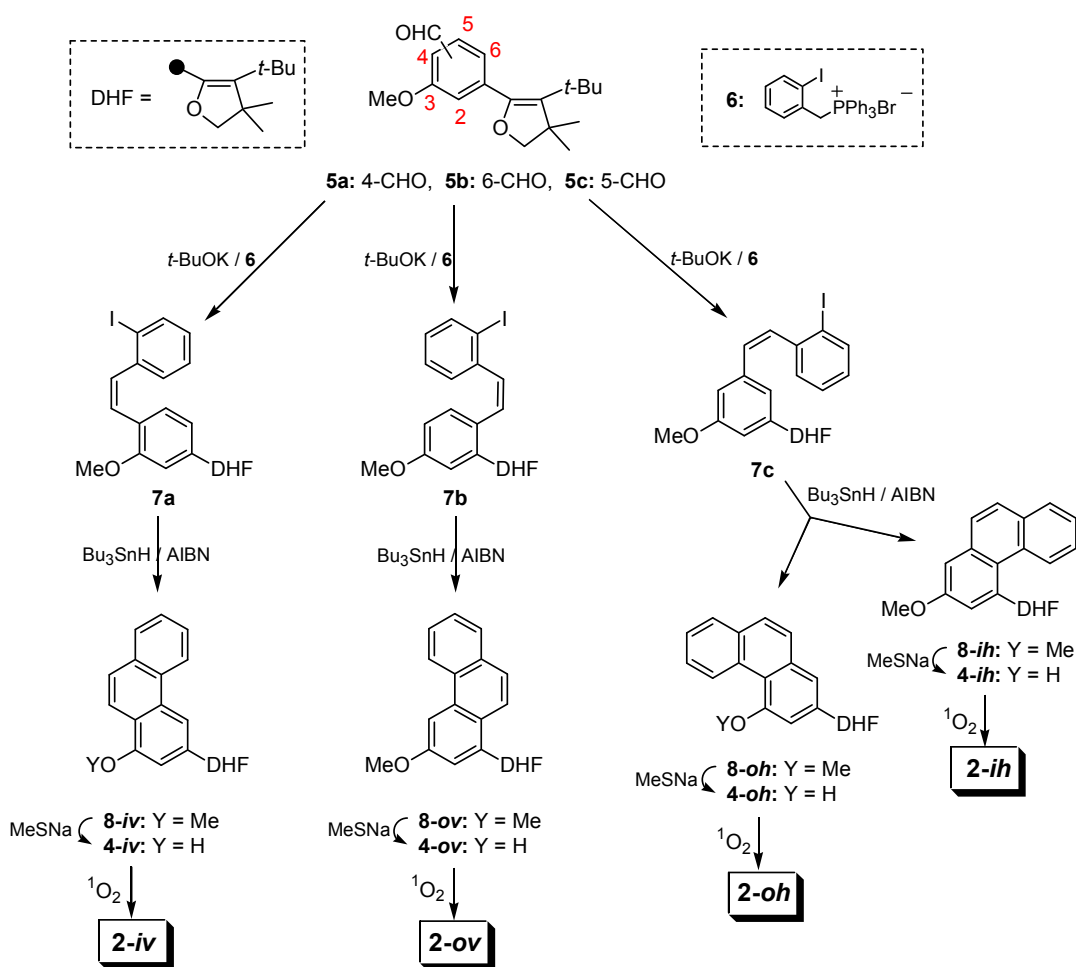
Bicyclic dioxetanes **2** bearing a hydroxyphenanthrene moiety were synthesized by singlet oxygenation of the corresponding dihydrofurans **4**. The key step in the synthesis of precursors **4** was the construction of di-substituted phenanthrene rings. Thus, we applied the cyclization of an *o*-halogeno-*Z*-stilbene using Bu₃SnH.¹⁴ The synthetic sequence leading to precursor **4-iv** for dioxetane **2-iv** is described here as a representative example (Scheme 1). First, we conducted a Wittig reaction of dihydrofuran **5a** bearing a 4-formyl-3-methoxyphenyl group with 2-iodobenzyltriphenylphosphorane prepared from phosphonium bromide **6** to give dihydrofuran **7a** bearing a 3-methoxyphenyl moiety substituted with a *Z*-(2-iodophenyl)ethenyl group at the 4-position in 96% yield along with a small amount of its *E*-isomer. When **7a** and Bu₃SnH were heated in the presence of AIBN (azobisisobutyronitrile) in toluene, the desired 1-methoxyphenanthren-3-yl-substituted dihydrofuran **8-iv** was produced in 85% isolated yield. Demethylation of a methoxy group in **8-iv** was attained by heating with sodium thiomethylate in DMF to give precursor **4-iv** in 99% yield.

As shown in Scheme 1, *Z*-stilbene-type compounds **7b** and **7c** were also prepared by the Wittig reaction of the corresponding aldehydes **5b** and **5c**. Cyclization of **7b** as for **7a** gave 3-methoxyphenanthrene **8-ov** in 86% yield, while the similar cyclization of **7c** gave 4-methoxyphenanthrene **8-oh** and its 2-methoxy-isomer **8-ih** in respective yields of 58% and 31%. These methoxyphenanthryl-substituted dihydrofurans **8-ov**, **8-oh** and **8-ih** were demethylated as in the case of **8-iv** to give the corresponding hydroxyphenanthryl-substituted dihydrofurans **4-ov**, **4-oh** and **4-ih** in yields of 87-98%.

When dihydrofuran **4-iv** was irradiated with a Na-lamp in the presence of a catalytic amount of tetraphenylporphyrin (TPP) in CH₂Cl₂ under an O₂ atmosphere at 0 °C, 1,2-addition of singlet oxygen to **4-iv** effectively proceeded to give thermally stable dioxetane **2-iv** in 78% isolated yield. Similar singlet oxygenation of precursors **4-ov** and **4-oh** smoothly took place to give thermally stable dioxetanes **2-ov** and **2-oh** in respective yields of 96% and 68%. On the other hand, singlet oxygenation of **4-ih** proceeded to mainly give keto ester **9-ih**, which was produced from thermally unstable dioxetane **2-ih**: all efforts to isolate pure **2-ih** were unsuccessful, so that we could obtain only a mixture of **2-ih** and **9-ih**. The structures of dioxetanes **2-iv**, **2-ov** and **2-oh** were determined by ¹H NMR, ¹³C NMR, IR, Mass and HRMass spectral analyses: the structure of **2-ih** was determined by ¹H NMR. All dioxetanes **2-iv**, **2-ov** and **2-oh** selectively gave the corresponding keto esters **9-iv**, **9-ov** and **9-oh** when heated in *p*-xylene (Figure 3).

Synthetic feasibility for dioxetanes **2-iv**, **2-ov**, **2-oh**, and **2-ih** suggested that the design of dioxetanes

bearing a hydroxyhelicene moiety appeared to be promising for the development of dioxetanes such as **2-iv** and **2-ov**. Thus, two selected dioxetanes bearing a hydroxy[4]helicene moiety **3-iv** and **3-ov** were synthesized according to a strategy similar to that for dioxetanes **2**. The precursor dihydrofurans **10-iv** and **10-ov** bearing a hydroxy[4]helicene moiety were synthesized starting from dihydrofurans **5a** and **5b**, respectively (Scheme 2). First, dihydrofurans **5a** and **5b** were reacted with a phosphorane prepared from phosphonium bromide **11** to give the corresponding *Z*-diarylethenes **12a** and **12b** in good yields. Cyclization of **12a** and **12b** was carried out as in the case of **7** to give the corresponding methoxy[4]helicene-substituted dihydrofurans **13-iv** and **13-ov** in respective yields of 45 and 62%. These



Scheme 1. Synthesis of bicyclic dioxetanes bearing a hydroxyphenanthrene moiety

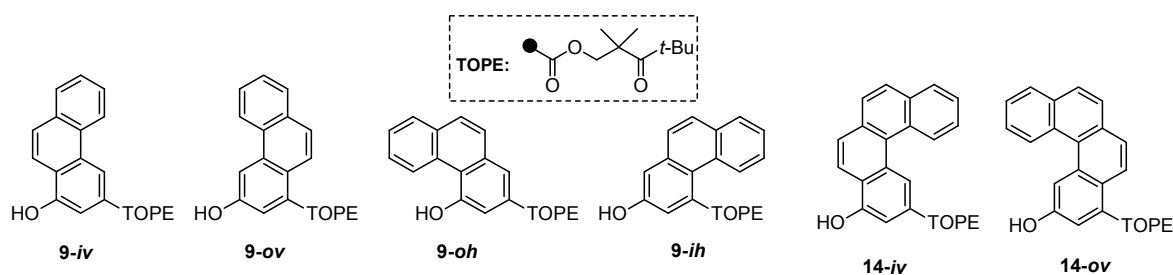
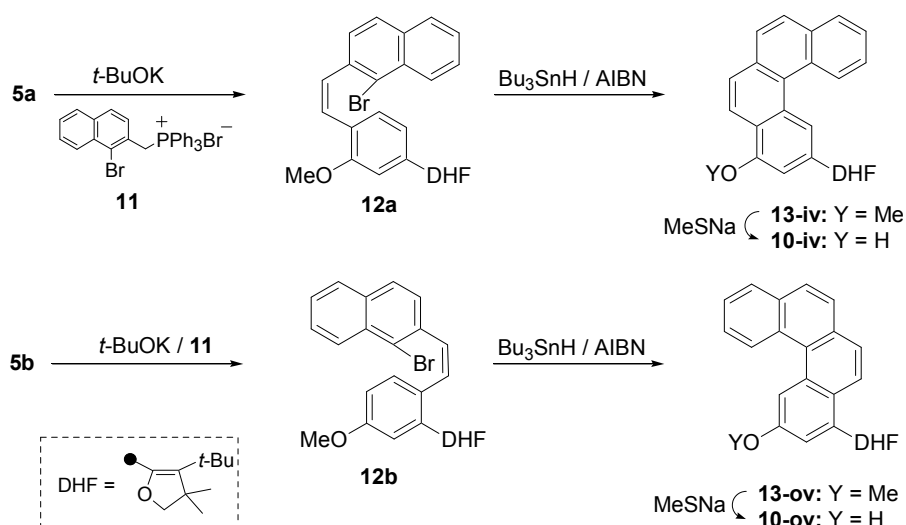


Figure 3. Hydroxyarene-carboxylic acid esters of 2,2,4,4-tetramethyl 3-oxopentanol

methoxyaryl-substituted dihydrofurans **13-iv** and **13-ov** were demethylated as in the case of **8-iv** to effectively give the precursor dihydrofurans **10-iv** and **10-ov**, respectively. Finally, singlet oxygenation of **10-iv** and **10-ov** was carried out at 0 °C to give dioxetanes **3-iv** and **3-ov** in respective yields of 60 and 86%. These dioxetanes were thermally stable, but selectively decomposed to the corresponding keto esters **14-iv** and **14-ov** under heating in *p*-xylene. Dioxetanes **3-iv** and **3-ov** gave satisfactory ¹H NMR, ¹³C NMR, Mass, and HRMass spectral data. Furthermore, X-ray single-crystallographic analysis was successfully performed for both dioxetanes **3-iv** and **3-ov**. Figure 4 shows their ORTEP views, from which we can infer that the [4]helicene ring is skewed by about 37°.



Scheme 2. Synthesis of bicyclic dioxetanes bearing a hydroxy[4]helicene moiety

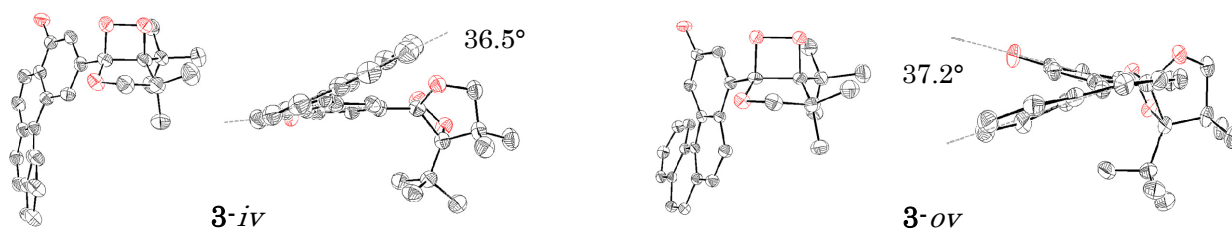
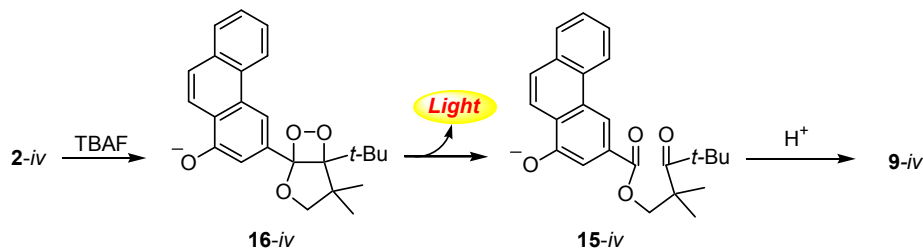


Figure 4. ORTEP views of bicyclic dioxetanes bearing a hydroxy[4]helicene moiety

Base-induced chemiluminescent decomposition of bicyclic dioxetanes bearing a hydroxyphenanthrene or hydroxy[4]helicene moiety

When a solution of **2-iv** in acetonitrile was added to a solution of tetrabutylammonium fluoride (TBAF, large excess) in acetonitrile at 25 °C, **2-iv** decomposed according to pseudo-first order kinetics independent of the TBAF concentration with an accompanying emission of yellow light, the spectrum of which is shown in Figure 6. The chemiluminescence properties of **2-iv** were as follows: maximum wavelength $\lambda_{\max}^{\text{CL}} = 506 \text{ nm}$, chemiluminescence efficiency $\Phi^{\text{CL}} = 5.2 \times 10^{-2}$,^{15,16} rate of CTID $k^{\text{CTID}} = 2.5 \text{ s}^{-1}$, and half-life $t_{1/2}^{\text{CTID}} = 0.28 \text{ s}$ (Table 1). The spent reaction mixture exclusively gave keto ester

9-iv after careful neutralization. Authentic oxido anion **15-iv** generated from **9-iv** in TBAF/acetonitrile gave fluorescence, the spectrum of which coincided with the chemiluminescence spectrum of **2-iv**. These results indicate that CTID of **2-iv** proceeded through an intermediary dioxetane **16-iv** to give anionic keto ester **15-iv** accompanied by the emission of light (Scheme 3). Thus, based on the fluorescence efficiency (Φ^{fl}) of **15-iv**, the chemiexcitation efficiency ($\Phi_{\text{S}} = \Phi^{\text{CL}}/\Phi^{\text{fl}}$) was estimated to be 0.10 (Table 1).



Scheme 3. TBAF-induced chemiluminescent decomposition of bicyclic dioxetane **2-iv**

Under similar treatment with TBAF in acetonitrile, **2-ov**, **2-oh**, and **2-ih** showed chemiluminescence, the spectra and properties of which are shown in Figure 6 and Table 1: **2-ih** was used as a mixture that included a large amount (ca. 30%) of **9-ih**. The chemiluminescence properties for dioxetanes **2** were compared to those for dioxetanes bearing a rather simple hydroxyaryl group, i.e., a 1-hydroxynaphthalen-3-yl **17a** or 3-hydroxynaphthalen-1-yl group **17b**, together with those for dioxetane **18** bearing a 3-hydroxyphenyl group (Figures 5 and 6 and Table 1): **17a** was synthesized according to the procedure for **17b**.^{9b} The data of Table 1 show that a) the Φ^{CL} values for all three of the hydroxyphenanthryl-substituted dioxetanes **2-iv**, **2-ov**, and **2-oh** were higher than or comparable to that for hydroxynaphthyl-substituted dioxetane **17b** though lower than that for **17a**, and b) the k^{CTID} values for dioxetanes bearing a β -naphthol-type arene moiety, i.e., **17b** and **2-ov**, were far lower than those for dioxetanes bearing an α -naphthol-type arene moiety, i.e., **17a**, **2-iv** and **2-oh**.

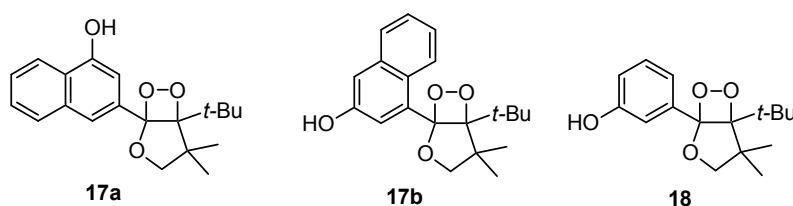


Figure 5. Bicyclic dioxetanes bearing a naphthol or phenol moiety

When dioxetane **3-iv** was treated with TBAF in acetonitrile as with **2**, **3-iv** decomposed to give a flash of yellow light with $\lambda_{\text{max}}^{\text{CL}} = 559 \text{ nm}$, the spectrum of which is shown in Figure 6 [A] together with those of **2-iv**, **2-ih**, **17a** and **18**. On the other hand, the TBAF-induced decomposition of **3-ov** showed a glowing light with $\lambda_{\text{max}}^{\text{CL}} = 530 \text{ nm}$, the spectrum of which is shown in Figure 6 [B] together with those of **2-oh**, **2-ov**, **17b** and **18**. The chemiluminescence properties for **3-iv** and **3-ov** are summarized in Table 1, which shows that their Φ^{CL} values were somewhat lower than that for **2-ov**. Thus, we attempted to

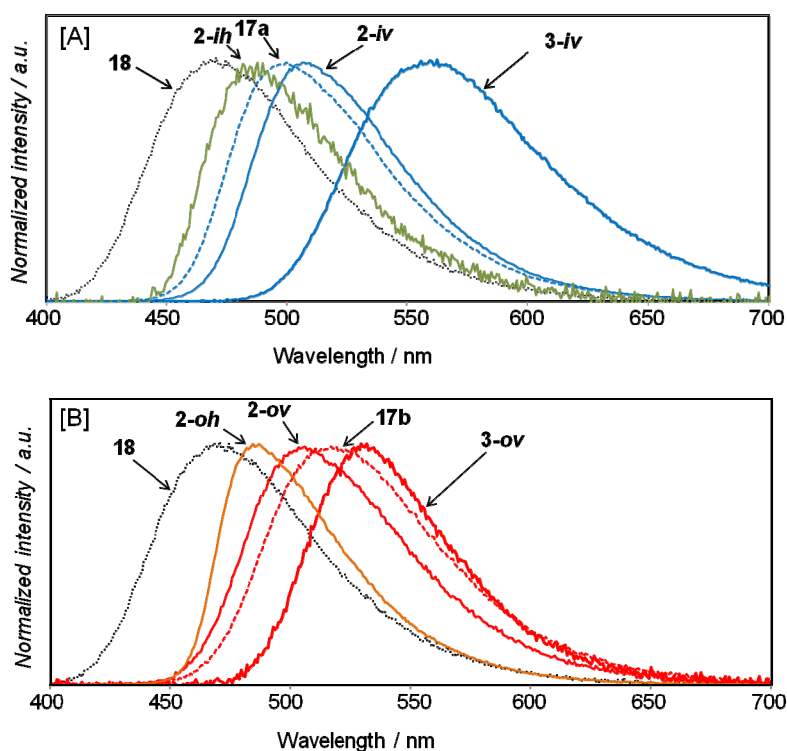


Figure 6. Chemiluminescence spectra for TBAF-induced decomposition of bicyclic dioxetanes bearing a hydroxyarene moiety

Table 1. Chemiluminescence properties of bicyclic dioxetanes bearing a hydroxyaryl moiety in a TBAF/acetonitrile system^{a)}

Dioxetane	λ_{\max} / nm	$\Phi^{\text{CL b)}$	Φ^{fl}	Φ_{S}	$k^{\text{CTID}} / \text{s}^{-1}$	$t_{1/2}^{\text{CTID}} / \text{s}$
17a	500	0.13	0.49	0.28	13	5.2×10^{-2}
2-iv	506	5.2×10^{-2}	0.52	0.10	2.5	0.28
2-oh	485	4.8×10^{-2}	0.23	0.21	0.46	1.5
3-iv	559	1.4×10^{-2}	0.22	0.07	3.6	0.19
17b^{c)}	515	2.6×10^{-2}	0.49	0.05	8.2×10^{-4}	850
2-ov	504	2.4×10^{-2}	0.29	0.08	6.3×10^{-4}	1100
2-ih	485	----- ^{d)}	----- ^{d)}	----- ^{d)}	----- ^{d)}	----- ^{d)}
3-ov	530	1.9×10^{-2}	0.36	0.05	1.8×10^{-3}	380
18^{e)}	471	0.11	0.24	0.46	2.8×10^{-2}	25

a) Unless stated otherwise, a solution of a dioxetane in MeCN (1.0×10^{-4} ~ 1.0×10^{-5} M, 1 mL) was added to a solution of TBAF in MeCN (1.0×10^{-2} M, 2 mL) at 25 °C. b) All of the Φ^{CL} values presented here were estimated based on the value reported for the chemiluminescent decomposition of 3-adamantylidene-4-(3-siloxyphenyl)-4-methoxy-1,2-dioxetane ($\Phi^{\text{CL}} = 0.29$) in TBAF/DMSO [Ref. 16]. c) [Ref. 9b] d) Not estimated. e) [Ref. 17]

understand how $\lambda_{\max}^{\text{CL}}$, k^{CTID} and Φ^{CL} changed with a change in the number of fused benzene rings from phenol to hydroxy[4]helicene for two series, i.e., the *iv*-series and *ov*-series, of hydroxyaryl-substituted dioxetanes, **18** → **17** → **2** → **3**.

Table 1 shows that $\lambda_{\max}^{\text{CL}}$ tended to shift to a longer wavelength region for both the *iv*-series and the *ov*-series as the number of fused benzene rings increased, with the exception of **2-ov**. This tendency may be due to the expansion of the π -conjugation system from oxidophenyl anion → oxidonaphthyl anion → oxidophenanthryl anion and finally to oxido[4]helicenyl anion. On the other hand, the k^{CTID} values for the *iv*-series were >1000 times larger than those for the *ov*-series regardless of the number of fused benzene rings. The significant difference in k^{CTID} values between the *iv*-series and *ov*-series is presumably attributed to the difference in the ease of oxidation of oxidoarene anions, which act as an electron donor for CTID. In fact, the anion of α -naphthol, corresponding to **17a**, has been reported to possess a formal oxidation potential ($E = -498$ mV vs Ag/Ag⁺ in DMSO) that is considerably lower than that of an anion of β -naphthol, corresponding to **17b** ($E = -369$ mV).¹⁸ This may also be the case for **2** and **3**: all of the dioxetanes in the *iv*-series have an α -naphthol-type arene moiety, while those in the *ov*-series have a β -naphthol-type arene moiety.

Table 1 further shows that the Φ_s value for a dioxetane bearing an α -naphthol-type arene (Table 1) tended to be higher than that for the corresponding dioxetane bearing a β -naphthol-type arene: **17a** >> **17b**, **2-oh** >> **2-iv** > **2-ov**, and **3-iv** > **3-ov**. This tendency can be explained by the “*syn/anti*” rotational isomerism of an aromatic electron donor, in which an *anti*-rotamer gives Φ_s far more effectively than a *syn*-rotamer (Scheme 4).^{19,20}

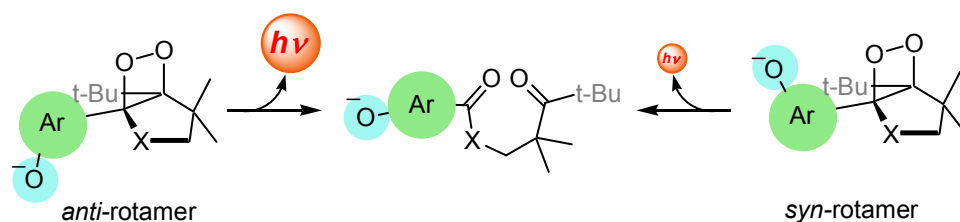
Table 2. Relationship between Φ_s and *syn/anti* rotational isomerism of an aromatic electron donor for the base-induced chemiluminescent decomposition of hydroxyaryl-substituted dioxetanes^{a)}

Dioxetane	Φ_s	$\Delta E_{\text{syn-anti}}$ /kcal mol ⁻¹	$\Delta E_{\text{rotation}}$ ^{b)} /kcal mol ⁻¹
18	0.46	-1.1	11.3, 13.5
17a	0.28	-1.7	9.9, 13.8
17b	0.05	1.1	13.3, 28.1
2-oh	0.21	-1.3	11.1, 13.3
2-iv	0.10	-1.2	11.5, 13.7
2-ov	0.08	0.6	13.8, 28.8
3-iv	0.07	-0.3	9.4, 15.0
3-ov	0.05	1.3	13.2, 28.3

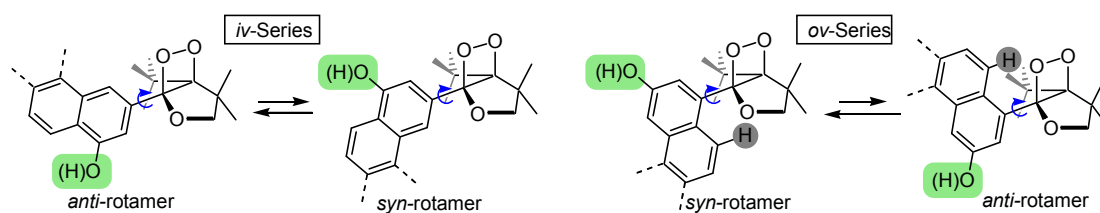
a) An oxido-anion form of dioxetane was calculated. b) Two energy barriers exist due to steric interaction of an aromatic ring to an oxygen of tetrahydrofuran ring as well as to *tert*-butyl group.

A *syn*-rotamer, typically shown in Figure 4, is likely to be more stable than an *anti*-rotamer for dioxetanes in the *ov*-series because of steric hindrance by a *peri*-hydrogen of an aromatic electron donor (Scheme 5). Thus, we carried out an MO calculation (Gaussian 03, HF/6-31G) to estimate the energy difference $\Delta E_{\text{anti-syn}}$ between the *syn*- and *anti*-rotamers and the barriers to rotation $\Delta E_{\text{rotation}}$ from the most stable rotamer

(*syn* or *anti*) to the other stable rotamer (*anti* or *syn*) (Table 2). The results show that a) the *syn*-rotamer is more stable than the *anti*-rotamer for the *ov*-series, while the *anti*-rotamer is more stable for the *iv*-series, and b) $\Delta E_{\text{rotation}}$ values for the *ov*-series tend to be higher than those for the *iv*-series. Thus, we can see that, for a dioxetane in the *iv*-series, the *anti*-rotamer is presumably predominant compared to the *syn*-rotamer, while a dioxetane in the *ov*-series shows the opposite tendency. Hence, a dioxetane in the *iv*-series would give a singlet-excited emitter more effectively than the corresponding dioxetane in the *ov*-series under these reaction conditions.



Scheme 4. Marked dependence of chemiluminescence efficiency on *syn/anti* rotational isomerism



Scheme 5. *syn/anti* Rotational isomerism of dioxetanes in *iv*-series and *ov*-series

CONCLUSION

Four bicyclic dioxetanes bearing a phenanthrene moiety possessing a hydroxy group in the A-ring **2-iv**, **2-ov**, **2-oh**, and **2-ih** were synthesized. Except for **2-ih**, these dioxetanes were thermally stable and underwent TBAF-induced decomposition with the accompanying emission of bright light. As an extension, we synthesized two dioxetanes **3-iv** and **3-ov** bearing a 4-hydroxy[4]helicen-2-yl or 2-hydroxy[4]helicen-4-yl group and found that their CTID effectively gave light. Thus, we investigated how the chemiluminescence properties of the *iv*-series and *ov*-series of dioxetanes changed with an increase in the number of fused benzene rings of a hydroxyarene moiety attached to a dioxetane ring. The results showed that a) $\lambda_{\text{max}}^{\text{CL}}$ tended to shift to a longer wave-length region for both the *iv*-series and the *ov*-series as the number of fused benzene rings increased, b) the k^{CTID} values for the *iv*-series were >1000 times larger than those for the *ov*-series regardless of the number of fused benzene rings, and c) the Φ_{S} value for a dioxetane bearing an α -naphthol-type arene (*iv*-series) tended to be higher than that for the

corresponding dioxetane bearing a β -naphthol-type arene (*ov*-series): **17a** >> **17b**, **2-oh** >> **2-iv** > **2-ov**, and **3-iv** > **3-ov**. This tendency could be explained by the “*syn/anti*” rotational isomerism of an aromatic electron donor, in which an *anti*-rotamer gives Φ_S far more effectively than a *syn*-rotamer.

EXPERIMENTAL

General

Melting points were uncorrected. IR spectra were taken on a FT/IR infrared spectrometer. ^1H and ^{13}C NMR spectra were recorded on a 300 MHz, 400 MHz and 500 MHz spectrometers. Mass spectra were obtained using double-focusing mass spectrometers and an ESI-TOF mass spectrometer. Column chromatography was carried out using silica gel.

Synthesis of 4-*tert*-butyl-5-{4-[*Z*-2-(2-iodophenyl)ethenyl]-3-methoxyphenyl}-3,3-dimethyl-2,3-dihydrofuran (**7a**): typical procedure.

Potassium *tert*-butoxide (1.82 g, 16.3 mmol) was added to a solution of 2-iodobenzyltriphenylphosphonium bromide (**6**) (7.43 g, 13.3 mmol) in dry THF (100 mL) under a nitrogen atmosphere at 0 °C and stirred for 30 min. To the solution was added dropwise 4-*tert*-butyl-5-(4-formyl-3-methoxyphenyl)-3,3-dimethyl-2,3-dihydrofuran (**5a**) (3.56 g, 12.4 mmol) in dry THF (90 mL) over 10 min at room temperature, and the mixture was stirred for 3 h. The reaction mixture was poured into H₂O and extracted with Et₂O. The organic layer was washed with sat. aq. NaCl, dried over anhydrous MgSO₄ and concentrated *in vacuo*. The residue was chromatographed on silica gel with AcOEt–hexane (1:4) to give **7a** (5.80 g, 11.9 mmol, 96%).

7a: colorless oil. ^1H NMR (400 MHz, CDCl₃): δ_{H} 1.03 (s, 9H), 1.31 (s, 6H), 3.81 (s, 3H), 3.86 (s, 2H), 6.56 (d, $J = 12.2$ Hz, 1H), 6.62 (dd, $J = 7.7$ and 1.4 Hz, 1H), 6.76 (s with fine coupling, 1H), 6.78 (d, $J = 12.2$ Hz, 1H), 6.82–6.88 (m, 1H), 6.87 (d, $J = 7.7$ Hz, 1H), 6.99–7.08 (m, 2H), 7.84 (dd, $J = 7.7$ and 1.0 Hz, 1H) ppm. ^{13}C NMR (125 MHz, CDCl₃): δ_{C} 27.4, 32.4, 32.4, 47.2, 55.5, 83.1, 99.8, 112.1, 122.0, 125.1, 125.8, 126.3, 127.7, 128.4, 129.6, 130.3, 134.1, 136.5, 138.8, 141.6, 149.7, 156.7 ppm. IR (liquid film): $\tilde{\nu}$ 3050, 2956, 2865, 1650, 1601, 1582, 1559 cm⁻¹. Mass (m/z , %): 488 (M⁺, 31), 474 (24), 473 (100), 363 (19), 345 (30), 215 (16), 165 (35). HRMS (ESI): 489.1303, calcd for C₂₅H₃₀IO₂ [M+H⁺] 489.1291; 511.1106, calcd for C₂₅H₂₉IO₂Na [M+Na⁺] 511.1110; 527.0849, calcd for C₂₅H₂₉IO₂K [M+K⁺] 527.0849.

7b: 57% yield. colorless columns, mp 76.5–77.0 °C (from AcOEt–hexane). ^1H NMR (500 MHz, CDCl₃): δ_{H} 1.10 (s, 9H), 1.37 (s, 6H), 3.76 (s, 3H), 3.91 (s, 2H), 6.44 (d, $J = 12.1$ Hz, 1H), 6.54 (dd, $J = 8.6$ and 2.8 Hz, 1H), 6.65 (d, $J = 12.1$ Hz, 1H), 6.77 (d, $J = 2.8$ Hz, 1H), 6.86–6.90 (m, 1H), 6.89 (d, $J = 8.6$ Hz, 1H), 7.10 (ddd, $J = 7.6$, 7.3 and 0.9 Hz, 1H), 7.16 (dd, $J = 7.6$ and 1.6 Hz, 1H), 7.87 (dd, $J = 8.0$ and 0.9 Hz, 1H) ppm. ^{13}C NMR (125 MHz, CDCl₃): δ_{C} 27.2, 32.1, 32.6, 47.2, 55.2, 83.2, 100.1, 113.7, 115.6, 126.6, 127.8, 128.1, 128.4, 128.9, 130.2, 130.3, 132.4, 137.2, 138.9, 141.8, 148.0, 158.3 ppm. IR (liquid film): $\tilde{\nu}$ 2963, 2860, 1604, 1564, 1461, 1307 cm⁻¹. Mass (m/z , %): 488 (M⁺, 38), 473 (28), 431 (17) 256 (7). HRMS (ESI): 511.1110, calcd for C₂₅H₂₉IO₂Na [M+Na⁺] 511.1110; 527.0861, calcd for C₂₅H₂₉IO₂K

[M+K⁺] 527.0849.

7c: 58% yield. colorless oil. ¹H NMR (400 MHz, CDCl₃): δ_H 0.98 (s, 9H), 1.28 (s, 6H), 3.59 (s, 3H), 3.82 (s, 2H), 6.52 (d, *J* = 12.0 Hz, 1H), 6.57 (dd, *J* = 2.4 and 1.3 Hz, 1H), 6.61 (d, *J* = 12.0 Hz, 1H), 6.64 (dd, *J* = 2.4 and 1.3 Hz, 1H), 6.67 (s with fine coupling, 1H), 6.87–6.92 (m, 1H), 7.11–7.18 (m, 2H), 7.85–7.88 (m, 1H) ppm. ¹³C NMR (125 MHz, CDCl₃): δ_C 27.3, 32.3, 32.5, 47.1, 55.0, 83.0, 99.5, 113.7, 114.8, 123.4, 125.5, 128.0, 128.6, 130.4, 130.8, 134.0, 137.1, 137.3, 139.0, 141.6, 149.4, 158.8 ppm. IR (liquid film): $\tilde{\nu}$ 2955, 2866, 1653, 1585, 1464 cm⁻¹. Mass (*m/z*, %): 488 (M⁺, 28), 474 (25), 473 (100). HRMS (ESI): 489.1292, calcd for C₂₅H₃₀IO₂ [M+H⁺] 489.1291; 511.1104, calcd for C₂₅H₂₉IO₂Na [M+Na⁺] 511.1110.

12a: 84% yield. colorless columns, mp 101.0–102.0 °C (from AcOEt–hexane). ¹H NMR (400 MHz, CDCl₃): δ_H 1.03 (s, 9H), 1.31 (s, 6H), 3.84 (s, 3H), 3.86 (s, 2H), 6.57 (dd, *J* = 7.8 and 1.4 Hz, 1H), 6.79 (d, *J* = 1.4 Hz, 1H), 6.90 (d, *J* = 7.8 Hz, 1H), 6.93 (s, 2H), 7.16 (d, *J* = 8.5 Hz, 1H), 7.45 (d, *J* = 8.5 Hz, 1H), 7.48 (dd with fine coupling, *J* = 8.0 and 6.9 Hz, 1H), 7.57 (dd with fine coupling, *J* = 8.5 and 6.9 Hz, 1H), 7.72 (d with fine coupling, *J* = 8.0 Hz, 1H), 8.34 (d with fine coupling, *J* = 8.5 Hz, 1H) ppm. ¹³C NMR (125 MHz, CDCl₃): δ_C 27.4, 32.4, 32.4, 47.1, 55.5, 83.1, 112.0, 121.9, 123.7, 125.2, 125.8, 126.3, 126.7, 126.8, 127.1, 127.1, 128.0, 128.2, 129.9, 130.7, 132.4, 133.5, 136.2, 136.7, 149.6, 156.7 ppm. IR (KBr): $\tilde{\nu}$ 2954, 2925, 2855, 1650, 1604, 1463 cm⁻¹. Mass (*m/z*, %): 492 (M⁺+2, 36), 490 (M⁺, 37), 478 (28), 477 (100), 475 (98), 395 (32), 367 (35), 365 (35), 340 (48), 215 (49). HRMS (ESI): 513.1399, calcd for C₂₉H₃₁⁷⁹BrO₂Na [M+Na⁺] 513.1405; 515.1387, calcd for C₂₉H₃₁⁸¹BrO₂Na [M+Na⁺] 515.1385.

12b: 72% yield. colorless columns, mp 129.0–130.0 °C (from Et₂O–hexane). ¹H NMR (500 MHz, CDCl₃): δ_H 1.12 (s, 9H), 1.39 (s, 6H), 3.75 (s, 3H), 3.93 (s, 2H), 6.49 (dd, *J* = 8.6 and 2.8 Hz, 1H), 6.78 (d, *J* = 12.1 Hz, 1H), 6.79 (d, *J* = 2.8 Hz, 1H), 6.81 (d, *J* = 12.1 Hz, 1H), 6.92 (d, *J* = 8.6 Hz, 1H), 7.25 (d, *J* = 8.6 Hz, 1H), 7.49 (dd with fine coupling, *J* = 7.9 and 6.9 Hz, 1H), 7.53 (d, *J* = 8.6 Hz, 1H), 7.57 (dd with fine coupling, *J* = 8.6 and 6.9 Hz, 1H), 7.74 (d, *J* = 7.9 Hz, 1H), 8.34 (d, *J* = 8.6 Hz, 1H) ppm. ¹³C NMR (125 MHz, CDCl₃): δ_C 27.3, 32.2, 32.6, 47.2, 55.2, 83.3, 113.7, 115.7, 123.8, 128.3, 126.3, 126.6, 127.0, 127.1, 127.2, 128.0, 128.3, 129.2, 129.4, 130.7, 132.5, 133.5, 136.6, 137.3, 148.0, 158.4 ppm. IR (KBr): $\tilde{\nu}$ 2956, 2863, 1602, 1487, 1049 cm⁻¹. Mass (*m/z*, %): 492 (M⁺+2, 1), 490 (M⁺, 1), 252 (1), 221 (4), 215 (5), 57 (100). HRMS (ESI): not observed.

Synthesis of 4-*tert*-butyl-5-(1-methoxyphenanthren-3-yl)-3,3-dimethyl-2,3-dihydrofuran (8-iv):

typical procedure. AIBN (177 mg, 1.08 mmol) and tributyltin hydride (3.40 mL, 12.6 mmol) were added to a solution of **7a** (2.57 g, 5.26 mmol) in dry toluene (180 mL) under a nitrogen atmosphere at room temperature, and the solution was stirred at 90 °C for 10 h. The reaction mixture was concentrated *in vacuo*. The residue was crystallized from AcOEt–hexane to give 4-*tert*-butyl-5-(1-methoxyphenanthren-3-yl)-3,3-dimethyl-2,3-dihydrofuran (**8-iv**) (1.61 g, 4.47 mmol, 85%).

8-iv: colorless columns, mp 141.0–142.0 °C (from Et₂O–hexane). ¹H NMR (400 MHz, CDCl₃): δ_H 1.11 (s, 9H), 1.42 (s, 6H), 3.98 (s, 2H), 4.05 (s, 3H), 6.93 (d, *J* = 1.0 Hz, 1H), 7.59 (dd with fine coupling, *J* = 7.7 and 6.9 Hz, 1H), 7.63 (dd with fine coupling, *J* = 8.2 and 6.9 Hz, 1H), 7.75 (d, *J* = 9.1 Hz, 1H), 7.89 (dd, *J* = 7.7 and 1.5 Hz, 1H), 8.21 (d, *J* = 9.1 Hz, 1H), 8.22 (s, 1H), 8.66 (d, *J* = 8.2 Hz, 1H) ppm. ¹³C

NMR (125 MHz, CDCl₃): δ_C 27.5, 32.5, 32.6, 47.3, 55.7, 83.1, 107.5, 116.7, 120.2, 122.8, 123.2, 126.0, 126.3, 126.4, 126.6, 128.5, 130.0, 130.9, 132.3, 134.4, 150.5, 155.5 ppm. IR (KBr): $\tilde{\nu}$ 2959, 2866, 1654, 1611, 1599 cm⁻¹. MASS (*m/z*, %): 360 (M⁺, 30), 346 (26), 345 (100), 289 (17), 235 (17), 57 (13). HRMS (ESI): 361.2168, calcd for C₂₅H₂₉O₂ [M+H⁺] 361.2168; 383.1991, calcd for C₂₅H₂₈O₂ Na [M+Na⁺] 383.1987; 415.2255, calcd for C₂₆H₃₂O₃Na [M+MeOH+Na⁺]415.2249.

8-ov: 86% yield. colorless columns, mp 136.0–137.0 °C (from AcOEt–hexane). ¹H NMR (500 MHz, CDCl₃): δ_H 1.01 (s, 9H), 1.43 (s, 3H), 1.49 (s, 3H), 4.02 (q_{AB}, *J* = 8.0 Hz, 2H), 4.02 (s, 3H), 7.21 (d, *J* = 2.4 Hz, 1H), 7.55–7.65 (m, 2H), 7.63 (d, *J* = 9.2 Hz, 1H), 7.81 (d, *J* = 9.2 Hz, 1H), 7.87 (dd, *J* = 7.6 and 1.1 Hz, 1H), 8.07 (d, *J* = 2.4 Hz, 1H), 8.60 (d, *J* = 8.0 Hz, 1H) ppm. ¹³C NMR (125 MHz, CDCl₃): δ_C 27.3, 27.6, 32.0, 32.6, 47.3, 55.5, 83.4, 104.6, 118.8, 122.8, 124.3, 124.9, 125.8, 126.1, 126.6, 127.9, 128.5, 129.8, 131.8, 132.3, 135.8, 147.6, 157.5 ppm. IR (liquid film): $\tilde{\nu}$ 2987, 2960, 2867, 1650, 1604, 1046 cm⁻¹. Mass (*m/z*, %): 360 (M⁺, 9), 345 (8), 288 (12), 245 (12), 235 (11), 215 (16), 202 (17), 57(100). HRMS (ESI): 361.2170, calcd for C₂₅H₂₉O₂ [M+H⁺] 361.2168; 383.1994, calcd for C₂₅H₂₈O₂Na [M+Na⁺] 383.1987.

8-oh: 58% yield. colorless columns, mp 113.5–114.0 °C (from AcOEt–hexane). ¹H NMR (300 MHz, CDCl₃): δ_H 1.10 (s, 9H), 1.40 (s, 6H), 3.96 (s, 2H), 4.15 (s, 3H), 7.08 (d, *J* = 1.5 Hz, 1H), 7.48 (d, *J* = 1.5 Hz, 1H), 7.54–7.67 (m, 2H), 7.68 (d, *J* = 8.7 Hz, 1H), 7.74 (d, *J* = 8.7 Hz, 1H) 7.87 (dd, *J* = 7.6 and 1.8 Hz, 1H), 9.64 (d with fine coupling, *J* = 8.1 Hz, 1H) ppm. ¹³C NMR (125 MHz, CDCl₃): δ_C 27.5, 32.5, 32.6, 47.3, 55.8, 83.3, 109.9, 120.4, 122.9, 126.0, 126.2, 126.4, 127.2, 128.1, 128.2, 128.6, 130.1, 132.9, 134.1, 134.3, 149.7, 158.4 ppm. IR (KBr): $\tilde{\nu}$ 3064, 2984, 2951, 1655, 1601, 1567 cm⁻¹. Mass (*m/z*, %): 360 (M⁺, 30), 346 (26), 345 (100), 289 (15), 235 (13). HRMS (ESI): 361.2179, calcd for C₂₅H₂₉O₂ [M+H⁺] 361.2168; 383.1985, calcd for C₂₅H₂₈O₂Na [M+Na⁺] 383.1987; 399.1771, calcd for C₂₅H₂₈O₂K [M+K⁺] 399.1726.

8-ih: 31% yield. colorless columns, mp 162.5–163.0 °C (from AcOEt–hexane). ¹H NMR (500 MHz, CDCl₃): δ_H 0.97 (s, 9H), 1.44 (s, 3H), 1.52 (s, 3H), 3.92 (s, 3H), 4.10(q_{AB}, *J* = 8.2 Hz, 2H) 7.18 (d, *J* = 2.9 Hz, 1H) 7.25 (d, *J* = 2.9 Hz, 1H), 7.50 (dd with fine coupling, *J* = 7.7 and 6.9 Hz, 1H), 7.54 (dd with fine coupling, *J* = 8.4 and 6.9 Hz, 1H) 7.62 (d, *J* = 8.8 Hz, 1H), 7.68 (d, *J* = 8.8 Hz, 1H), 7.82 (d with fine coupling, *J* = 7.7 Hz, 1H), 9.16 (d, *J* = 8.4 Hz, 1H) ppm. ¹³C NMR (125 MHz, CDCl₃): δ_C 26.2, 27.9, 31.7, 32.7, 47.1, 55.4, 83.7, 110.0, 122.1, 123.4, 124.0, 125.4, 125.7, 126.4, 127.1, 127.9, 128.4, 130.5, 132.0, 134.3, 134.9, 151.1, 156.6 ppm. IR (KBr): $\tilde{\nu}$ 3051, 2956, 2867, 1641, 1600, 1575, 1263, 1231, 1202 cm⁻¹. Mass (*m/z*, %): 360 (M⁺, 28), 346 (25), 345 (100), 303 (13), 289 (14), 235 (12). HRMS (ESI): 361.2187, calcd for C₂₅H₂₉O₂ [M+H⁺] 361.2168; 383.1989, calcd for C₂₅H₂₈O₂Na [M+Na⁺] 383.1987; 399.1758, calcd for C₂₅H₂₈O₂K [M+K⁺] 399.1726.

13-iv: 45% yield. colorless columns, mp 170.0–171.0 °C. (from CH₂Cl₂–hexane). ¹H NMR (300 MHz, CDCl₃): δ_H 1.15 (s, 9H), 1.41 (s, 6H), 3.96 (s, 2H), 4.10 (s, 3H), 6.94 (d, *J* = 1.0 Hz, 1H), 7.57–7.69 (m, 2H), 7.82 (d, *J* = 8.5 Hz, 1H), 7.83 (d, *J* = 8.8 Hz, 1H), 7.89 (d, *J* = 8.5 Hz, 1H), 8.00 (dd, *J* = 7.5 and 1.8 Hz, 1H), 8.39 (d, *J* = 8.8 Hz, 1H), 8.64 (s with fine coupling, 1H), 9.87 (d with fine coupling, *J* = 8.1 Hz, 1H) ppm. ¹³C NMR (125 MHz, CDCl₃): δ_C 27.5, 32.6, 32.6, 47.3, 55.8, 83.2, 106.5, 120.8, 121.9, 124.7,

125.7, 125.9, 126.0, 126.4, 126.8, 127.2, 127.6, 128.1, 128.4, 130.4, 130.8, 131.4, 133.5, 134.1, 150.7, 155.4 ppm. IR (KBr): $\tilde{\nu}$ 2958, 2866, 1652, 1601 cm^{-1} . Mass (m/z , %): 410 (M^+ , 38), 396 (28), 395 (100), 339 (15), 285 (11), 242 (11), 214 (10). HRMS (ESI): 411.2331, calcd for $\text{C}_{29}\text{H}_{31}\text{O}_2$ [$M+H^+$] 411.2324; 433.2149, calcd for $\text{C}_{29}\text{H}_{30}\text{O}_2\text{Na}$ [$M+\text{Na}^+$] 433.2144.

13-ov: 62% yield. colorless needles, mp 136.0–136.5 °C. (from CH_2Cl_2 –hexane). ^1H NMR (500 MHz, CDCl_3): δ_{H} 1.05 (s, 9H), 1.45 (s, 3H), 1.51 (s, 3H), 4.01 (s, 3H), 4.04 (q_{AB}, $J = 8.1$ Hz, 2H), 7.26 (d, $J = 2.5$ Hz, 1H), 7.60 (dd with fine coupling, $J = 7.9$ and 6.8 Hz, 1H), 7.66 (dd with fine coupling, $J = 8.5$ and 6.8 Hz, 1H), 7.72 (d, $J = 8.6$ Hz, 1H), 7.79 (d, $J = 8.5$ Hz, 1H), 7.87 (d, $J = 8.5$ Hz, 1H), 7.98 (d, $J = 8.6$ Hz, 1H), 8.01 (d with fine coupling, $J = 7.9$ Hz, 1H), 8.57 (d, $J = 2.5$ Hz, 1H), 9.16 (d, $J = 8.5$ Hz, 1H) ppm. ^{13}C NMR (125 MHz, CDCl_3): δ_{C} 27.3, 27.6, 32.0, 32.7, 47.4, 55.6, 83.4, 109.8, 118.6, 125.0 (x 2), 125.6, 125.9, 126.8, 126.9, 127.2, 127.5, 127.5, 128.0, 128.6, 130.5, 131.4, 131.7, 133.4, 135.5, 147.8, 157.2 ppm. IR (KBr): $\tilde{\nu}$ 3052, 2956, 2862, 1648, 1601 cm^{-1} . Mass (m/z , %): 410 (M^+ , 100), 396 (18), 395 (60), 380 (15), 365 (16), 339 (15). HRMS (ESI): 411.2324, calcd for $\text{C}_{29}\text{H}_{31}\text{O}_2$ [$M+H^+$] 411.2324; 433.2147, calcd for $\text{C}_{29}\text{H}_{30}\text{O}_2\text{Na}$ [$M+\text{Na}^+$] 433.2144.

Synthesis of 4-tert-butyl-5-(1-hydroxyphenanthren-3-yl)-3,3-dimethyl-2,3-dihydrofuran (4-iv) : typical procedure. Sodium thiomethoxide (119 mg, 1.70 mmol) was added to a solution of **8-iv** (301 mg, 0.835 mmol) in dry DMF (10 mL) and stirred under a nitrogen atmosphere at 150 °C for 30 min. The reaction mixture was poured into sat. aq. NH_4Cl and extracted with AcOEt. The organic layer was washed with sat. aq. NaCl, dried over anhydrous MgSO_4 and concentrated *in vacuo*. The residue was chromatographed on silica gel with AcOEt–hexane (5:1) to give **4-iv** (286 mg, 0.854 mmol, 99%).

4-iv: colorless columns, mp 218.0–218.5 °C (from Et_2O –hexane). ^1H NMR (400 MHz, CDCl_3): δ_{H} 1.10 (s, 9H), 1.41 (s, 6H), 3.97 (s, 2H), 5.40 (s, 1H), 6.92 (d, $J = 1.2$ Hz, 1H), 7.56–7.66 (m, 2H), 7.72 (d, $J = 9.0$ Hz, 1H), 7.88 (d with fine coupling, $J = 7.6$ Hz, 1H), 8.09 (dd, $J = 9.0$ and 0.6 Hz, 1H), 8.22 (s, 1H), 8.64 (d, $J = 8.1$ Hz, 1H) ppm. ^{13}C NMR (125 MHz, CDCl_3): δ_{C} 27.4, 32.6, 32.6, 47.3, 83.2, 112.6, 117.1, 119.9, 121.8, 123.2, 126.3, 126.4, 126.5, 126.6, 128.5, 130.0, 131.2, 132.2, 133.9, 149.8, 151.6 ppm. IR (KBr): $\tilde{\nu}$ 3333, 2955, 2869, 1654, 1614, 1601 cm^{-1} . MASS (m/z , %): 346 (M^+ , 29), 332 (24), 331 (100), 275 (17), 221 (20), 165 (14). HRMS (ESI): 369.1831, calcd for $\text{C}_{24}\text{H}_{26}\text{O}_2\text{Na}$ [$M+\text{Na}^+$] 369.1831; 385.1574, calcd for $\text{C}_{24}\text{H}_{26}\text{O}_2\text{K}$ [$M+\text{K}^+$] 385.1570.

4-ov: 97% yield. colorless columns, mp 139.0–139.5 °C (from CH_2Cl_2 –hexane). ^1H NMR (300 MHz, CDCl_3): δ_{H} 1.01 (s, 9H), 1.43 (s, 3H), 1.50 (s, 3H), 4.02 (q_{AB}, $J = 8.1$ Hz, 2H), 5.11 (s, 1H), 7.13 (d, $J = 2.4$ Hz, 1H), 7.54–7.61 (m, 2H), 7.62 (d, $J = 8.9$ Hz, 1H), 7.79 (d, $J = 8.9$ Hz, 1H), 7.82–7.87 (m, 1H), 8.00 (d, $J = 2.4$ Hz, 1H), 8.47–8.52 (m, 1H) ppm. ^{13}C NMR (125 MHz, CDCl_3): δ_{C} 27.3, 27.4, 31.9, 32.6, 47.3, 83.3, 107.8, 119.3, 122.8, 124.1, 124.9, 125.6, 126.1, 126.6, 128.3, 128.4, 129.5, 132.0, 132.2, 135.4, 147.2, 153.4 ppm. IR (KBr): $\tilde{\nu}$ 3311, 2983, 2967, 2870, 1653, 1614, 1602 cm^{-1} . Mass (m/z , %): 346 (M^+ , 3), 221 (10), 165 (49), 164 (13), 163 (15), 95 (25), 57 (100). HRMS (ESI): 369.1835, calcd for $\text{C}_{24}\text{H}_{26}\text{O}_2\text{Na}$ [$M+\text{Na}^+$] 369.1831; 385.1579, calcd for $\text{C}_{24}\text{H}_{26}\text{O}_2\text{K}$ [$M+\text{K}^+$] 385.1570.

4-oh: 98% yield. colorless columns, mp 179.5–180.0 °C (from AcOEt–hexane). ^1H NMR (300 MHz, CDCl_3): δ_{H} 1.10 (s, 9H), 1.39 (s, 6H), 3.94 (s, 2H), 5.77 (s, 1H), 6.95 (d, $J = 1.5$ Hz, 1H), 7.46 (d, $J = 1.5$

Hz, 1H), 7.54–7.68 (m, 2H), 7.66 (d, $J = 8.9$ Hz, 1H), 7.72 (d, $J = 8.9$ Hz, 1H), 7.87 (d with fine coupling, $J = 7.6$ Hz, 1H), 9.61 (d with fine coupling, $J = 8.3$ Hz, 1H) ppm. ^{13}C NMR (125 MHz, CDCl_3): δ_{C} 27.4, 32.5, 32.6, 47.3, 83.1, 114.9, 119.3, 122.9, 126.0, 126.4, 126.9 (broad), 127.0, 128.0, 128.1, 128.6, 130.1, 132.6, 133.7 (broad), 134.4, 149.1, 154.2 ppm. IR (KBr): $\tilde{\nu}$ 3212, 3061, 2956, 2866, 1661, 1610, 1599, 1570 cm^{-1} . Mass (m/z , %): 346 (M^+ , 31), 332 (24), 331 (100), 275 (16), 221 (16), 165 (11). HRMS (ESI): 347.2016, calcd for $\text{C}_{24}\text{H}_{27}\text{O}_2$ [$\text{M}+\text{H}^+$] 347.2011; 369.1829, calcd for $\text{C}_{24}\text{H}_{26}\text{O}_2\text{Na}$ [$\text{M}+\text{Na}^+$] 369.1831. 385.1584, calcd for $\text{C}_{24}\text{H}_{26}\text{O}_2\text{K}$ [$\text{M}+\text{K}^+$] 385.1570.

4-ih: 87% yield. colorless columns, mp 155.5–156.0 °C (from CH_2Cl_2 –hexane). ^1H NMR (500 MHz, CDCl_3): δ_{H} 0.95 (s, 9H), 1.44 (s, 3H), 1.52 (s, 3H), 4.13 (q_{AB}, $J = 8.3$ Hz, 2H) 5.87 (broad s, 1H), 6.91 (dd, $J = 4.7$ and 2.7 Hz, 1H), 7.07 (d, $J = 2.8$ Hz, 1H), 7.31 (dd, $J = 8.8$ and 4.7 Hz, 1H), 7.50 (dd with fine coupling, $J = 7.7$ and 6.9 Hz, 1H), 7.54 (dd with fine coupling, $J = 8.4$ and 6.9 Hz, 1H), 7.60 (d, $J = 8.8$ Hz, 1H), 7.80 (dd, $J = 7.7$ and 1.4 Hz, 1H), 9.13 (d, $J = 8.4$ Hz, 1H) ppm. ^{13}C NMR (125 MHz, CDCl_3): δ_{C} 26.1, 27.9, 31.6, 32.7, 47.1, 83.6, 113.4, 122.0, 123.3, 124.4, 125.5, 125.7, 126.3, 126.9, 127.9, 128.5, 130.4, 132.0, 133.9, 134.9, 150.6, 152.6 ppm. IR (KBr): $\tilde{\nu}$ 3347, 3049, 2977, 2953, 2869, 1640, 1617, 1571 cm^{-1} . Mass (m/z , %): 346 (M^+ , 27), 332 (24), 331 (100), 289 (13), 275 (11), 221 (12), 165 (11). HRMS (ESI): 369.1829, calcd for $\text{C}_{24}\text{H}_{26}\text{O}_2\text{Na}$ [$\text{M}+\text{Na}^+$] 369.1831.

10-iv: 91% yield. colorless columns, mp 155.5–156.0 °C (from CH_2Cl_2 –hexane). ^1H NMR (300 MHz, CDCl_3): δ_{H} 1.16 (s, 9H), 1.40 (s, 6H), 3.95 (s, 2H) 5.41 (broad s, 1H), 6.94 (d, $J = 1.2$ Hz, 1H), 7.58–7.70 (m, 2H), 7.81 (d, $J = 8.4$ Hz, 1H), 7.81 (d, $J = 8.8$ Hz, 1H), 7.90 (d, $J = 8.4$ Hz, 1H), 8.01 (d with fine coupling, $J = 7.4$ Hz, 1H), 8.28 (d with fine coupling, $J = 8.8$ Hz, 1H), 8.65 (d, $J = 1.2$ Hz, 1H), 9.08 (d with fine coupling, $J = 8.0$ Hz, 1H) ppm. ^{13}C NMR (125 MHz, CDCl_3): δ_{C} 27.4, 32.5, 32.6, 47.2, 83.0, 111.7, 120.6, 122.2, 123.8, 125.7, 125.9, 126.2, 126.6, 126.8, 127.2, 127.5, 128.1, 128.4, 130.4, 131.0, 131.3, 133.4, 133.4, 150.0, 151.6 ppm. IR (KBr): $\tilde{\nu}$ 3396, 2957, 2921, 2868, 1651. 1606 cm^{-1} . Mass (m/z , %): 396 (M^+ , 34), 382 (28), 381 (100), 325 (15), 271 (14), 215 (10). HRMS (ESI): 397.2178, calcd for $\text{C}_{28}\text{H}_{29}\text{O}_2$ [$\text{M}+\text{H}^+$] 397.2168; 419.1989, calcd for [$\text{M}+\text{Na}^+$] 419.1987.

10-ov: 86% yield. colorless columns, mp 169.0–170.0 °C (from AcOEt –hexane). ^1H NMR (500 MHz, CDCl_3): δ_{H} 1.04 (s, 9H), 1.44 (s, 3H), 1.51 (s, 3H), 4.05 (q_{AB}, $J = 8.0$ Hz, 2H), 5.39 (s, 1H), 7.17 (d, $J = 2.5$ Hz, 1H), 7.57 (dd with fine coupling, $J = 7.8$ and 6.9 Hz, 1H), 7.61 (dd with fine coupling, $J = 8.3$ and 6.9 Hz, 1H), 7.68 (d, $J = 8.8$ Hz, 1H), 7.76 (d, $J = 8.5$ Hz, 1H), 7.84 (d, $J = 8.5$ Hz, 1H), 7.95 (d, $J = 8.8$ Hz, 1H), 7.97 (d with fine coupling, $J = 7.8$ Hz, 1H), 8.46 (d, $J = 2.5$ Hz, 1H), 9.03 (d, $J = 8.3$ Hz, 1H) ppm. ^{13}C NMR (125 MHz, CDCl_3): δ_{C} 27.3, 27.4, 31.9, 32.7, 47.3, 83.3, 112.6, 118.8, 124.7, 124.9, 125.5, 125.9, 126.3, 126.7, 127.3, 127.3, 127.5, 128.4, 128.4, 130.4, 131.3, 131.8, 133.2, 135.2, 147.4, 153.2 ppm. IR (KBr): $\tilde{\nu}$ 3348, 3051, 2958, 2869, 1650, 1603 cm^{-1} . Mass (m/z , %): 396 (M^+ , 2), 324 (10), 295 (4), 271 (12), 226 (11), 215 (33), 213 (37), 57 (100). HRMS (ESI): 419.1992, calcd for $\text{C}_{28}\text{H}_{28}\text{O}_2\text{Na}$ [$\text{M}+\text{Na}^+$] 419.1987; 435.1741, calcd for $\text{C}_{28}\text{H}_{28}\text{O}_2\text{K}$ [$\text{M}+\text{K}^+$] 435.1726.

Synthesis of 5-tert-butyl-1-(1-hydroxyphenanthren-3-yl)-4,4-dimethyl-2,6,7-trioxabicyclo[3.2.0]heptane (2-iv) : typical procedure. A solution of **4-iv** (201 mg, 0.580 mmol) and tetraphenylporphyrin (TPP) (2.0 mg) in CH_2Cl_2 (20 mL) was irradiated externally with a 940 W Na lamp

under an O₂ atmosphere at 0 °C for 35 min. The residue was chromatographed on silica gel with Et₂O–hexane (1:9) to give **2-iv** (171 mg, 0.452 mmol, 78%) to give colorless solid.

2-iv: colorless columns, mp 99.5–100.5 °C (from Et₂O–hexane). ¹H NMR (400 MHz, CDCl₃): δ_H 1.02 (s, 9H), 1.21 (s, 3H), 1.47 (s, 3H), 3.91 (d, *J* = 8.2 Hz, 1H), 4.68 (d, *J* = 8.2 Hz, 1H), 5.53 (s, 1H), 7.21 (s, 1H), 7.62 (dd with fine coupling, *J* = 7.8 and 7.0 Hz, 1H), 7.67 (dd with fine coupling, *J* = 8.2 and 7.0 Hz, 1H), 7.80 (d, *J* = 9.1 Hz, 1H), 7.91 (dd, *J* = 7.8 and 1.1 Hz, 1H), 8.13 (d, *J* = 9.1 Hz, 1H), 8.61 (s, 1H), 8.71 (d, *J* = 8.2 Hz, 1H) ppm. ¹³C NMR (125 MHz, CDCl₃): δ_C 18.5, 25.2, 26.9, 36.9, 45.7, 80.3, 105.2, 110.1, 116.1, 116.9, 119.7, 122.5, 123.3, 126.9, 127.0, 127.4, 128.7, 130.2, 131.1, 132.3, 134.1, 151.7 ppm. IR (KBr): $\tilde{\nu}$ 3419, 3238, 2979, 2895, 1620, 1603, 1576 cm⁻¹. Mass (*m/z*, %): 378 (M⁺, 20), 322 (18), 238 (36), 221 (100) 193 (16), 165 (26), 57 (41). HRMS (ESI): 401.1734, calcd for C₂₄H₂₆O₄Na [M+Na⁺] 401.1729.

2-ov: 96% yield. colorless columns, mp 163.0–163.5 °C (from CH₂Cl₂–hexane). ¹H NMR (500 MHz, CDCl₃): δ_H 0.92 (s, 9H), 1.32 (s, 3H), 1.67 (s, 3H), 4.12 (d, *J* = 8.7 Hz, 1H), 4.72 (d, *J* = 8.7 Hz, 1H), 5.17 (broad s 1H), 7.57–7.65 (m, 2H), 7.63 (d, *J* = 9.4 Hz, 1H), 7.83–7.87 (m, 1H), 7.97 (broad, 1H), 8.21 (d, *J* = 2.8 Hz, 1H), 8.38–8.48 (m, 1H), 8.57 (d, *J* = 7.8 Hz, 1H) ppm. ¹³C NMR (125 MHz, CDCl₃): δ_C 20.2, 26.2, 26.8, 36.9, 45.7, 80.8, 106.5, 109.3, 117.3, 120.2, 123.1, 124.3, 124.4, 124.9, 126.4, 127.0, 128.2, 129.8, 131.6, 133.2, 133.9, 153.1 ppm. IR(KBr): $\tilde{\nu}$ 3452, 2975, 2891, 1614, 1405, 1217 cm⁻¹. Mass (*m/z*, %): 378 (M⁺, 39), 322 (20), 238 (50), 222 (16), 221 (100). HRMS (ESI): 401.1726, calcd for C₂₄H₂₆O₄Na [M+Na⁺] 401.1729; 417.1504, calcd for C₂₄H₂₆O₄K [M+K⁺] 417.1468.

2-oh: 68% yield. pale yellow columns, mp 140.5–141.5 °C (from CH₂Cl₂–hexane). ¹H NMR (400 MHz, CDCl₃): δ_H 1.02 (s, 9H), 1.20 (s, 3H), 1.46 (s, 3H), 3.90 (d, *J* = 8.3 Hz, 1H), 4.66 (d, *J* = 8.3 Hz, 1H), 5.83 (s, 1H), 7.25 (d, *J* = 1.6 Hz, 1H), 7.59–7.70 (m, 2H), 7.73 (d, *J* = 8.9 Hz, 1H), 7.77 (d, *J* = 8.9 Hz, 1H), 7.80 (d, *J* = 1.6 Hz, 1H), 7.90 (d with fine coupling, *J* = 7.8 Hz, 1H), 9.64 (d with fine coupling, *J* = 8.4 Hz, 1H) ppm. ¹³C NMR (125 MHz, CDCl₃): δ_C 18.5, 25.1, 26.9, 36.8, 45.7, 80.3, 105.3, 112.5, 116.6, 120.1, 121.8, 126.4, 126.7, 127.3, 128.2, 128.5, 128.7, 129.9, 133.0, 133.8, 134.3, 154.3 ppm. IR (KBr): $\tilde{\nu}$ 3245, 3051, 2968, 1627, 1574, 1402 cm⁻¹. Mass (*m/z*, %): 378 (M⁺, 24), 322 (19), 238 (39), 222 (17), 221 (100), 193 (19), 165 (51). HRMS (ESI): 401.1719, calcd for C₂₄H₂₆O₄Na [M+Na⁺] 401.1729.

3-iv: 60% yield. pale yellow columns mp 190.0–91.0 °C (from CH₂Cl₂–hexane). ¹H NMR (300 MHz, CDCl₃): δ_H 1.07 (s, 9H), 1.21 (s, 3H), 1.50 (s, 3H), 3.89 (d, *J* = 8.2 Hz, 1H), 4.67 (d with fine coupling, *J* = 8.2 Hz, 1H), 5.49 (s 1H), 7.25 (broad d, *J* = 1.1 Hz, 1H), 7.59–7.70 (m, 2H), 7.83 (d, *J* = 8.5 Hz, 1H), 7.89 (d, *J* = 8.8 Hz, 1H), 7.92 (d, *J* = 8.5 Hz, 1H), 7.99–8.05 (m, 1H), 8.33 (d with fine coupling, *J* = 8.8 Hz, 1H), 9.01–9.07 (m, 2H) ppm. ¹³C NMR (125 MHz, CDCl₃): δ_C 18.5, 25.0, 27.0, 36.9, 45.7, 80.3, 105.5, 109.1, 117.2, 120.5, 121.0, 124.3, 126.0, 126.2, 126.7, 127.2, 127.5, 127.9 (x 2), 128.5, 130.3, 130.8, 131.5, 133.5, 133.6, 151.8 ppm. IR (KBr): $\tilde{\nu}$ 3439, 3052, 3005, 2964, 2898, 1613, 1603, 1413 cm⁻¹. Mass (*m/z*, %): 428 (M⁺, 62), 372 (31), 288 (39), 272 (22), 271 (100), 57 (43). HRMS (ESI): 451.1895, calcd for C₂₈H₂₈O₄Na [M+Na⁺] 451.1885.

3-ov: 86% yield. pale yellow columns, mp 192.0–193.0 °C (from AcOEt–hexane). ¹H NMR (400 MHz, CDCl₃): δ_H 0.95 (s, 9H), 1.33 (s, 3H), 1.69 (s, 3H), 4.14 (d, *J* = 8.5 Hz, 1H), 4.74 (d, *J* = 8.5 Hz, 1H), 5.21

(s 1H), 7.58–7.70 (m, 2H), 7.70 (d, $J = 9.0$ Hz, 1H), 7.77 (d, $J = 8.5$ Hz, 1H), 7.89 (d, $J = 8.5$ Hz, 1H), 7.96–8.03 (m, 1H), 8.00 (dd, $J = 7.9$ and 1.3 Hz, 1H), 8.56–8.64 (m, 1H), 8.62 (d, $J = 2.2$ Hz, 1H), 9.04 (d, $J = 8.3$ Hz, 1H) ppm. ^{13}C NMR (125 MHz, CDCl_3): δ_{C} 20.2, 26.2, 26.9, 37.0, 45.7, 80.8, 106.4, 114.3, 119.9, 124.4, 124.8, 125.8, 126.2, 126.4, 126.6, 126.8, 127.7, 128.0, 128.6, 127.7, 128.0, 128.6, 130.4, 130.7, 132.9, 133.4, 133.6, 152.6 ppm. IR (KBr): $\tilde{\nu}$ 3460, 3050, 2998, 2977, 2896, 1616 cm^{-1} . Mass (m/z , %): 428 (M^+ , 63), 372 (24), 288 (58) 272 (22), 271 (100), 215 (30), 57 (30). HRMS (ESI): 429.2110, calcd for $\text{C}_{28}\text{H}_{29}\text{O}_4$ [$\text{M}+\text{H}^+$] 429.2066; 451.1876, calcd for $\text{C}_{28}\text{H}_{28}\text{O}_4\text{Na}$ [$\text{M}+\text{Na}^+$] 451.1885.

Synthesis of 2,2,4,4-tetramethyl-3-oxopentyl 1-hydroxyphenanthrene-3-carboxylate (9-iv): typical procedure. TBAF (1M in THF, 0.75 mL, 0.75 mmol) in MeCN (1.5 mL) was added to a solution of **2-iv** (57.0 mg, 0.151 mmol) in MeCN (1.5 mL) and stirred for 5 min. The reaction mixture was poured into sat. aq. NH_4Cl and extracted with AcOEt. The organic layer was washed with sat. aq. NaCl, dried over anhydrous MgSO_4 and concentrated *in vacuo*. The residue was chromatographed on silica gel and recrystallization with Et_2O –hexane (1:3) gave **9-iv** (53.0 mg, 0.140 mmol, 93%).

9-iv: pale yellow needles, mp 164.5–165.0 °C (from CH_2Cl_2 –hexane). ^1H NMR (400 MHz, CDCl_3): δ_{H} 1.35 (s, 9H), 1.47 (s, 6H), 4.53 (s, 2H), 6.13 (s, 1H), 7.58 (s with fine coupling, 1H), 7.64 (dd with fine coupling, $J = 7.3$ and 7.1 Hz, 1H), 7.69 (dd with fine coupling, $J = 8.2$ and 7.1 Hz, 1H), 7.86 (d, $J = 9.1$ Hz, 1H), 7.92 (d, $J = 7.3$ Hz, 1H), 8.18 (d, $J = 9.1$ Hz, 1H), 8.67 (d, $J = 8.2$ Hz, 1H), 8.96 (s, 1H) ppm. ^{13}C NMR (125 MHz, CDCl_3): δ_{C} 23.8, 28.2, 46.0, 49.5, 72.4, 110.0, 117.0, 120.1, 123.0, 125.3, 127.0, 127.1, 127.4, 128.5, 128.7, 130.3, 131.1, 132.2, 152.8, 167.0, 217.1 ppm. IR (KBr): $\tilde{\nu}$ 3433, 2971, 1695, 1604, 1274 cm^{-1} . Mass (m/z , %): 378 (M^+ , 31), 322 (24), 238 (36), 222 (16), 221 (100), 193 (13), 165 (20), 57 (31). HRMS (ESI): 401.1741, calcd for $\text{C}_{24}\text{H}_{26}\text{O}_4\text{Na}$ [$\text{M}+\text{Na}^+$] 401.1729.

9-ov: colorless columns, mp 163.0–163.5 °C (from CH_2Cl_2 –hexane). ^1H NMR (400 MHz, CDCl_3): δ_{H} 1.29 (s, 9H), 1.44 (s, 6H), 4.51 (s, 2H), 5.90 (s, 1H), 7.58–7.66 (m, 2H), 7.69 (d, $J = 2.6$ Hz, 1H), 7.69 (d, $J = 9.4$ Hz, 1H), 7.84–7.90 (m, 1H), 8.28 (d, $J = 2.6$ Hz, 1H), 8.52–8.57 (m, 1H), 8.63 (d, $J = 9.4$ Hz, 1H) ppm. ^{13}C NMR (125 MHz, CDCl_3): δ_{C} 23.7, 28.2, 46.0, 49.3, 72.5, 111.7, 119.5, 122.8, 123.5, 125.3, 126.3, 126.4, 127.1, 128.4, 129.2, 129.5, 131.9, 132.8, 153.1, 167.2, 216.9 ppm. IR (KBr): $\tilde{\nu}$ 3420, 2965, 2928, 1714, 1674, 1620, 1229 cm^{-1} . Mass (m/z , %): 378 (M^+ , 40), 322 (21), 238 (50), 222 (16), 221 (100), 165 (33), 57 (22). HRMS (ESI): 401.1728, calcd for $\text{C}_{24}\text{H}_{26}\text{O}_4\text{Na}$ [$\text{M}+\text{Na}^+$] 401.1729.

9-oh: yellow columns, mp 163.0–163.5 °C (from CH_2Cl_2 –hexane). ^1H NMR (400 MHz, CDCl_3): δ_{H} 1.33 (s, 9H), 1.45 (s, 6H), 4.51 (s, 2H), 6.35 (broad s, 1H), 7.60 (d, $J = 1.6$ Hz, 1H), 7.62 (dd with fine coupling, $J = 7.8$ and 7.0 Hz, 1H), 7.67 (dd with fine coupling, $J = 8.3$ and 7.0 Hz, 1H), 7.73 (d, $J = 8.9$ Hz, 1H), 7.78 (d, $J = 8.9$ Hz, 1H), 7.91 (dd, $J = 7.4$ and 1.6 Hz, 1H), 8.13 (d, $J = 1.6$ Hz, 1H), 9.70 (d, $J = 8.4$ Hz, 1H) ppm. ^{13}C NMR (125 MHz, CDCl_3): δ_{C} 23.7, 28.2, 46.0, 49.4, 72.4, 112.7, 122.9, 123.0, 126.7, 126.9, 127.1, 127.4, 128.2, 128.6, 129.1, 130.0, 133.4, 134.2, 155.5, 166.9, 217.2 ppm. IR (KBr): $\tilde{\nu}$ 3356, 2976, 1720, 1690, 1669, 1227 cm^{-1} . Mass (m/z , %): 378 (M^+ , 1), 238 (2), 221 (4), 165 (18), 163 (11), 57 (100). HRMS (ESI): 401.1728, calcd for $\text{C}_{24}\text{H}_{26}\text{O}_4\text{Na}$ [$\text{M}+\text{Na}^+$] 401.1729.

9-ih: colorless columns, mp 148.5–149.0 °C (from CH_2Cl_2 –hexane). ^1H NMR (400 MHz, CDCl_3): δ_{H} 1.07 (s, 9H), 1.29 (s, 6H), 4.99 (s, 2H), 5.48 (broad s, 1H), 7.25 (d, $J = 2.7$ Hz, 1H), 7.30 (d, $J = 8.8$ Hz,

1H), 7.81–7.85 (m, 1H), 8.07–8.11 (m, 1H) ppm. ^{13}C NMR (125 MHz, CDCl_3): δ_{C} 23.6, 27.7, 45.8, 48.9, 73.7, 114.6, 117.8, 121.6, 125.5, 125.9, 126.0, 126.4, 128.4, 128.5, 128.9, 131.9, 134.8, 153.3, 171.9, 216.7 ppm. IR (KBr): $\tilde{\nu}$ 3371, 2981, 2875, 1720, 1667, 1621 cm^{-1} . Mass (m/z , %): 378 (M^+ , 1), 221 (4) 193 (6), 165 (19), 57 (100). HRMS (ESI): 401.1733, calcd for $\text{C}_{24}\text{H}_{26}\text{O}_4\text{Na}$ [$\text{M}+\text{Na}^+$] 401.1729.

14-iv: yellow needles, mp 197.0–198.0 °C (from AcOEt–hexane). ^1H NMR (400 MHz, CDCl_3): δ_{H} 1.27 (s, 9H), 1.46 (s, 6H), 4.53 (s, 2H), 5.95 (broad s, 1H), 7.60 (d, $J = 1.3$ Hz, 1H), 7.66 (dd with fine coupling, $J = 7.9$ and 7.0 Hz, 1H), 7.76 (dd with fine coupling, $J = 8.5$ and 7.0 Hz, 1H), 7.84 (d, $J = 8.5$ Hz, 1H), 7.94 (d, $J = 8.5$ Hz, 1H), 7.95 (d, $J = 8.8$ Hz, 1H), 8.03 (dd, $J = 7.9$ and 1.4 Hz, 1H), 8.37 (d with fine coupling, $J = 8.8$ Hz, 1H), 9.05 (d, $J = 8.5$ Hz, 1H), 9.44 (s with fine coupling, 1H) ppm. ^{13}C NMR (125 MHz, CDCl_3): δ_{C} 23.6, 28.3, 45.9, 49.4, 72.1, 108.8, 120.8, 122.9, 126.1, 126.6, 126.6, 126.8, 127.0, 127.8, 128.0, 128.1, 128.5, 128.5, 130.1, 130.8, 131.4, 133.6, 152.7, 167.3, 216.8 ppm. IR (KBr): $\tilde{\nu}$ 3416, 3048, 2976, 2964, 1698, 1603, 1418, 1278 cm^{-1} . Mass (m/z , %): 428 (M^+ , 58), 372 (30), 288 (43), 272 (20), 271 (100), 243 (16), 242 (11), 215 (18), 213 (15), 57 (28). HRMS (ESI): 451.1888, calcd for $\text{C}_{28}\text{H}_{28}\text{O}_4\text{Na}$ [$\text{M}+\text{Na}^+$] 451.1885.

14-ov: colorless columns, mp 133.0–133.5 °C (from CH_2Cl_2 –hexane). ^1H NMR (500 MHz, CDCl_3): δ_{H} 1.30 (s, 9H), 1.45 (s, 6H), 4.53 (s, 2H), 5.84 (s, 1H), 7.60 (ddd, $J = 7.8$, 6.9 and 1.1 Hz, 1H), 7.65 (ddd, $J = 8.2$, 6.9 and 1.6 Hz, 1H), 7.75 (d, $J = 8.9$ Hz, 1H), 7.77 (d, $J = 2.5$ Hz, 1H), 7.78 (d, $J = 8.5$ Hz, 1H), 7.90 (d, $J = 8.5$ Hz, 1H), 8.00 (dd, $J = 7.8$ and 1.6 Hz, 1H), 8.70 (d, $J = 2.5$ Hz, 1H), 8.75 (d, $J = 8.9$ Hz, 1H), 8.96 (d, $J = 8.2$ Hz, 1H) ppm. ^{13}C NMR (125 MHz, CDCl_3): δ_{C} 23.7, 28.2, 46.0, 49.3, 72.5, 116.6, 119.3, 124.3, 125.8, 126.2, 126.3, 126.3, 126.5, 126.9, 127.4, 128.1, 128.6, 129.2, 130.2, 131.1, 132.5, 133.4, 152.7, 167.2, 216.6 ppm. IR (KBr): $\tilde{\nu}$ 3341, 2979, 2959, 1687, 1603, 1210 cm^{-1} . Mass (m/z , %): 428 (M^+ , 61), 372 (23), 289 (12), 288 (57), 272 (22), 271 (100), 243 (11), 242 (11), 215 (30), 213 (17), 57 (25). HRMS (ESI): 451.1878, calcd for $\text{C}_{28}\text{H}_{28}\text{O}_4\text{Na}$ [$\text{M}+\text{Na}^+$] 451.1885.

Chemiluminescence measurement and time-course for the charge-transfer-induced decomposition of dioxetane. general procedure: Chemiluminescence was measured using a spectrophotometer and/or a multi-channel detector.

A freshly prepared solution (2.0 mL) of TBAF (1.0×10^{-2} mol dm^{-3}) in MeCN was transferred to a quartz cell (10 x 10 x 50 mm) and the latter was placed in a spectrometer, which was thermostated with stirring at 25 °C. After ca. 1 min, a solution of dioxetane **2** or **3** in MeCN (1.0×10^{-4} or 1.0×10^{-5} mol dm^{-3} , 1.0 mL) was added by a syringe, and measurement was started immediately. The time-course of the intensity of light emission was recorded and processed according to first-order kinetics. The total light emission was estimated by comparing it to that of an adamantylidene-dioxetane, the chemiluminescence efficiency Φ^{CL} of which has been reported to be 0.29 and which was used here as a standard.^{15,16}

Fluorescence Measurement of Authentic Emitters 9 and 14: A freshly prepared solution of 2.0×10^{-5} ~ 3.0×10^{-4} mol dm^{-3} of **9** or **14** and 1.0×10^{-3} mol dm^{-3} of TBAF in MeCN was transferred to a quartz cell (10 x 10 x 50 mm), and the latter was placed in the spectrometer, which was thermostated with stirring at 25 °C. Thus, the fluorescence spectra of **9** and **14** were measured and their fluorescence efficiencies (Φ^{fl}) were estimated using quinine hydrosulfate as a standard.

X-Ray single crystallographic analysis of **3-iv** and **3-ov**

X-Ray diffraction data were collected on a Rigaku Mercury CCD diffractometer with graphite monochromated Mo K α ($\lambda=0.71070$ Å) radiation. Data were processed using CrystalClear.[†] The structures were solved by direct method (SIR2008)[‡] and expanded using Fourier techniques. The non-hydrogen atoms were refined anisotropically. Hydrogen atoms were refined using the riding model. The final cycle of full-matrix least-squares refinement on F^2 was based on 5094 observed reflections and 318 variable parameters (for **3-iv**) and on 5009 observed reflections and 318 variable parameters (for **3-ov**). All calculations were performed using the CrystalStructure crystallographic software package.^{§,¶}

† Rigaku Corporation, 1999.

‡ SIR2008: M.C. Burla, R. Caliendo, M. Camalli, B. Carrozzini, G.L. Cascarano, L. De Caro, C. Giacovazzo, G. Polidori, D. Siliqi, R. Spagna (2007).

§ CrystalStructure 4.0: Crystal Structure Analysis Package, Rigaku Corporation (2000-2010). Tokyo 196-8666, Japan.

¶ CRYSTALS Issue 11: Carruthers, J.R., Rollett, J.S., Betteridge, P.W., Kinna, D., Pearce, L., Larsen, A., and Gabe, E. Chemical Crystallography Laboratory, Oxford, UK. (1999).

Crystal data for **3-iv**: C₂₈H₂₈O₄ ($M_r = 428.53$), pale yellow block, 0.12 x 0.10 x 0.05 mm, monoclinic, space group $P2_{1/c}$ (#14), $a = 16.45(5)$ Å, $b = 12.31(2)$ Å, $c = 11.029(17)$ Å, $\beta = 90.101(19)^\circ$, $V = 2233(9)$ Å³, $Z = 4$, $\rho_{\text{calcd}} = 1.274$ g cm⁻³, $T = 120$ K, $F(000) = 912.00$, reflections collected/unique 23562 / 5094 ($R_{\text{int}} = 0.0587$), $\mu(\text{MoK}\alpha) = 0.84$ cm⁻¹. An empirical absorption correction was applied which resulted in transmission factors ranging from 0.898 – 1.0000. The data were corrected for Lorentz and polarization effects. $R1 = 0.062$ [$I > 2\sigma(I)$], $wR2 = 0.186$ (all data) GOF on $F^2 = 1.004$, and residual electron density 0.43 / -0.43 e⁻Å⁻³.

Crystal data for **3-ov**: C₂₈H₂₈O₄ ($M_r = 428.53$), pale yellow prism, 0.15 x 0.10 x 0.07 mm, monoclinic, space group $P2_{1/c}$ (#14), $a = 16.75(3)$ Å, $b = 12.336(11)$ Å, $c = 11.202(12)$ Å, $\beta = 108.40(13)^\circ$, $V = 2196(5)$ Å³, $Z = 4$, $\rho_{\text{calcd}} = 1.296$ g cm⁻³, $T = 120$ K, $F(000) = 912.00$, reflections collected/unique 22506 / 5009 ($R_{\text{int}} = 0.051$), $\mu(\text{MoK}\alpha) = 0.854$ cm⁻¹. An empirical absorption correction was applied which resulted in transmission factors ranging from 0.923 – 1.0000. The data were corrected for Lorentz and polarization effects. $R1 = 0.0454$ [$I > 2\sigma(I)$], $wR2 = 0.0984$ (all data) GOF on $F^2 = 1.002$, and residual electron density 0.34 / -0.33 e⁻Å⁻³.

Crystallographic data for the structural analysis of compound **3-iv** and **3-ov** have been deposited at the Cambridge Crystallographic Data Center, CCDC-989777 and CCDC-989778. Copies of the data can be obtained, free of charge, on application to CCDC, 12 Union Road, Cambridge CB2 1EZ, UK, (fax: +44-(0)1223-336033 or e-mail: deposit@ccdc.cam.ac.uk).

ACKNOWLEDGEMENTS

We gratefully acknowledge financial assistance provided by Grants-in-aid (No. 25350269 No. 25410056

and No. 25410057) for Scientific Research from the Ministry of Education, Culture, Sports, Science, and Technology, Japan.

REFERENCES AND NOTES

1. A. P. Schaap and S. D. Gagnon, *J. Am. Chem. Soc.*, 1982, **104**, 3504.
2. (a) A. P. Schaap, R. S. Handley, and B. P. Giri, *Tetrahedron Lett.*, 1987, **28**, 935; (b) A. P. Schaap, T. S. Chen, R. S. Handley, R. DeSilva, and B. P. Giri, *Tetrahedron Lett.*, 1987, **28**, 1155.
3. (a) S. Beck and H. Köster, *Anal. Chem.*, 1990, **62**, 2258; (b) W. Adam, D. Reihardt, and C. R. Saha-Möller, *Analyst.*, 1996, **121**, 1527; (c) M. Matsumoto, *J. Photochemphotobiol. C: Photochem. Rev.*, 2004, **5**, 27; (d) M. Matsumoto and N. Watanabe, *Bull. Chem. Soc. Jpn.*, 2005, **78**, 1899.
4. (a) W. Adam and A. V. Trofimov, In *The Chemistry of Peroxides*; ed. by Z. Rappoport; Wiley: New York, 2006; Vol. 2, pp. 1171–1209; (b) W. J. Baader, C. V. Stevani, and E. L. Bastos, In *The Chemistry of Peroxides*; ed. by Z. Rappoport; Wiley: New York, 2006; Vol. 2, pp. 1211–1278.
5. (a) A. V. Trofimov, R. F. Vasil'ev, K. Mielke, and W. Adam, *Photochem Photobiol.*, 1995, **62**, 35; (b) W. Adam, I. Bronstein, B. Edwards, T. Engel, D. Reinhardt, F. W. Schneider, A. V. Trofimov, and R. F. Vasil'ev, *J. Am. Chem. Soc.*, 1996, **118**, 10400; (c) W. Adam, I. Bronstein, A. V. Trofimov, and R. F. Vasil'ev, *J. Am. Chem. Soc.*, 1999, **121**, 958.
6. (a) M. Matsumoto, N. Watanabe, N. C. Kasuga, F. Hamada, and K. Tadokoro, *Tetrahedron Lett.*, 1997, **38**, 2863; (b) W. Adam, M. Matsumoto, and A. V. Trofimov, *J. Am. Chem. Soc.*, 2000, **122**, 8631.
7. (a) I. Bronstein, B. Edwards, and J. C. Voyta, *J. Biolumin. Chemilumin.*, 1989, **4**, 99; (b) A. P. Schaap, H. Akhavan, and R. J. Romano, *Clin. Chem.*, 1989, **35**, 1863.
8. M. Yamada, K. Kitaoka, M. Matsumoto, and N. Watanabe, In *Bioluminescence and Chemiluminescence*, ed. by A. Tsuji, M. Matsumoto, M. Maeda, L. J. Kricka, and P. E. Stanley; World Scientific: Singapore, 2004; pp. 487–490.
9. (a) M. Matsumoto, K. Hamaoka, Y. Takashima, M. Yokokawa, K. Yamada, N. Watanabe, and H. K. Ijuin, *Chem. Commun.*, 2005, 808; (b) N. Hoshiya, N. Watanabe, H. K. Ijuin, and M. Matsumoto, *Tetrahedron*, 2006, **62**, 12424.
10. M. Matsumoto, N. Watanabe, N. Hoshiya, and H. K. Ijuin, *Chem. Rec.*, 2008, **8**, 213.
11. (a) B. Edward, A. Sparks, J. C. Voyta, and I. Bronstein, *J. Biolumin. Chemilumin.*, 1990, **5**, 1; (b) B. Edward, A. Sparks, J. C. Voyta, Strong, O. Murphy, and I. Bronstein, *J. Org. Chem.*, 1990, **55**, 6225; (c) N. Watanabe, H. Kobayashi, M. Azami, and M. Matsumoto, *Tetrahedron*, 1999, **55**, 6831; (d) N. Hoshiya, N. Hukuda, H. Maeda, N. Watanabe, and M. Matsumoto, *Tetrahedron*, 2006, **62**, 5808.
12. An “odd/even” relationship between the chemiluminescence properties and substitution pattern of a trigger group for CTID of oxyaryl-substituted dioxetanes was initially observed for dioxetanes bearing a 6- or 7-oxynaphthyl group. An “odd” pattern is one which the donor’s ($-O^-$) point of attachment to the acceptor (dioxetane ring) is such that the total number of ring carbon atoms

separating these points, including the atoms at the point of attachment, is an odd whole number [Refs. 11(a) and 11(b)].

13. For convenience, we refer to the four hydroxyphenanthryl-substituted dioxetanes investigated here as follows. For the structural formula shown in Figure 2, there are two types of isomers, i.e., one **2-*v*** possesses a phenanthrene C ring that lies *vertically* and the other **2-*h*** has a ring that lies *horizontally* with respect to the dioxetane ring. Second, these two isomers can each be separated into two isomers in which the helix of the phenanthrene ring is oriented *inner* or *outer* with respect to the dioxetane ring. Thus, there are four possible types, i.e., **2-*iv***, **2-*ov***, **2-*oh***, and **2-*ih***, for dioxetane **2**. A similar discussion can be applied to dioxetanes **3-*iv***, and **3-*ov***.
14. C. D. Harrowven, L. L. Guy, and L. Nanson, *Angew. Chem. Int. Ed.*, 2006, **45**, 2242.
15. All of the Φ^{CL} values presented here were estimated based on the value reported for the chemiluminescent decomposition of 3-adamantylidene-4-(3-siloxyphenyl)-4-methoxy-1,2-dioxetane ($\Phi^{\text{CL}} = 0.29$) in TBAF/DMSO.¹⁶
16. A. V. Trofimov, K. Mielke, R. F. Vasil'ev, and W. Adam, *Photochem. Photobiol.*, 1996, **63**, 463.
17. M. Matsumoto, Y. Mizoguchi, T. Motoyama, and N. Watanabe, *Tetrahedron Lett.*, 2001, **42**, 88692.
18. A. Nishinaga, M. Yano, T. Kuwashige, K. Maruyama, and T. Mashino, *Chem. Lett.*, 1994, 817.
19. For convenience sake, we call a rotamer an *anti*-form when the dioxetane O-O and a hydroxy group on an aromatic ring are on opposite sides of the furan ring, while in the *syn*-form the dioxetane O-O and a hydroxy group on an aromatic ring are on the same side of the furan ring.
20. (a) M. Matsumoto, H. Suzuki, N. Watanabe, H. K. Ijuin, J. Tanaka, and C. Tanaka, *J. Org. Chem.*, 2011, **76**, 5006; (b) N. Watanabe, K. Matsumoto, T. Tanaka, H. Suzuki, H. K. Ijuin, and M. Matsumoto, *Tetrahedron Lett.*, 2012, **53**, 5309.